Restricted Motion of Photoexcited Bacteriorhodopsin in Purple Membrane Containing Ethanol

Takashi Kikukawa,* Tsunehisa Araiso,* Tateo Shimozawa,# Kôichi Mukasa,§ and Naoki Kamo¶
*Center for Advanced Science and Technology, #Research Institute for Electronic Science, §Faculty of Engineering and ¶Pharmaceutical Sciences, Hokkaido University, Sapporo 060, Japan

ABSTRACT The molecular motion of retinal within the purple membrane was investigated by flash-induced absorption anisotropies with or without ethanol. In the absence of ethanol, the measured anisotropies at several wavelengths exhibited almost the same slow decay. This slow decay was attributed to only the rotation of purple membrane sheet itself in the aqueous suspension. In the presence of ethanol, however, we observed the wavelength-dependent anisotropies. The fluidity of the purple membrane, investigated with a fluorescence anisotropy method, was increased by the addition of ethanol. These facts indicated that the characteristic motion of bacteriorhodopsin is induced in perturbed purple membrane with ethanol. The data analysis was performed, taking account of the overlapping of absorption from ground-state bacteriorhodopsin and photointermediates. The results showed that the rotational motion of photointermediates within the membrane was more restricted than that of nonexcited bacteriorhodopsin. The addition of ethanol facilitated the rotation of nonexcited protein, whereas it did not significantly affect the motion of photointermediates. The restricted motion of photointermediates is probably caused by a conformational change in them, which may hinder the rotation of monomer protein and/or induce the interaction between photointermediate and neighboring proteins.

INTRODUCTION

Bacteriorhodopsin (bR), the sole pigment in the purple membrane of *Halobacterium salinarium*, functions as a light-driven proton pump. When light is absorbed by all-*trans* retinal, which is bound to the apoprotein via a protonated Schiff base linkage, bR initiates the photochemical cycle, which includes several intermediates. This cyclic reaction accomplishes a proton translocation across the cell membrane.

For each intermediate, the protonation states of the Schiff base and the conformation of retinal have been well investigated. Many aspects of the charged states of individual amino acids at each intermediate have also been characterized. These studies have provided evidence for "micro" conformational changes inside the protein, and the accumulated knowledge has encouraged researchers to propose models for the proton pumping mechanism (see, for reviews, Henderson et al., 1990; El-Sayed, 1992; Oesterhelt et al., 1992; Rothschild, 1992; Lanyi, 1993). Besides these studies on micro conformational changes, the measurement of dynamics of the retinal and/or protein motion within the membrane should offer new information on the mechanism of protein function. The wobbling motion of retinal inside the protein and/or the rotational motion of whole protein within the membrane is probably affected by the conformational change in the protein. To detect such a motion, flash-induced absorption anisotropy becomes a powerful tool.

Reported results from absorption anisotropy, however, are contradictory. Sherman and Caplan (1977) noted the temperature dependence of flash-induced anisotropy decay in the purple membrane aqueous suspension and suggested the displacement of the absorption dipole in the photointermediate. A few investigators detected wavelength-dependent anisotropy changes in purple membranes suspended in buffer solutions (Ahl and Cone, 1984; Wan et al., 1993; Song et al., 1994). They suggested the possibility of rotational motion of the whole protein during the photochemical cycle. Contrary to these studies, other investigators have not found detectable motion of the chromophore within the purple membrane (Sherman et al., 1976; Cherry et al., 1977; Korenstein and Hess, 1978; Stoeckenius et al., 1979; Kouyama et al., 1981). They attributed the slow decay of the measured anisotropies to the rotational motion of the purple membrane sheet itself. Moreover, Otto and Heyn (1991) and Otto et al. (1995) reported that the angular deviations of absorption dipoles between ground-state bR and M- or O-intermediates are only a few degrees.

This contradiction may be caused by the tight packing of bR in the purple membrane. bR molecules are arranged in a hexagonal lattice as trimmers in the membrane (Henderson and Unwin, 1975), and the membrane fluidity is very small (Kinosita et al., 1981). Within the rigid membrane, the molecular motion of retinal and/or the rotational motion of whole protein must be small. Under this situation, the small difference in measuring and/or preparation condition for the purple membrane may lead to different results. For mutant D96N (Asp-96 of wild-type bR is replaced with Asn), however, we observed wavelength-dependent anisotropy changes (Kikukawa et al., 1995). The lifetime of M-inter-

Received for publication 2 December 1996 and in final form 16 April 1997.
Address reprint requests to Dr. Takashi Kikukawa, Center for Advanced Science and Technology, Hokkaido University, Sapporo 060, Japan. Tel.: +81-11-706-7199; Fax: +81-11-706-7220; E-mail: kikukawa@cast.hokudai.ac.jp.

0006-3495/97/07/357/10 $2.00

mediate of D96N is very slow with respect to that of wild-type bR. Thus a simple condition is provided for the comparison of motion between nonexcited bR and the M-intermediate, and we concluded that the rotational motion of nonexcited bR within the membrane is faster than that of the M-intermediate. The site-specific mutation should affect the protein conformation and may disturb the tight packing of bR, and so the rotation of nonexcited bR may become measurable. Then we considered a working hypothesis that a perturbation of the rigid membrane of wild-type bR would enhance the motion of protein within the membrane.

Mitaku et al. (1988) reported the disruption of hydrogen bonds between helix coils in bR by the addition of alcohol. The hydrogen bonding interaction was considered to stabilize the protein structure. Fukuda and Kouyama (1992) found an alteration in photochemical kinetics in the presence of alcohol. They attributed this alteration to the softening of protein conformation. Moreover, it has been reported that alcohol affects the structure and physical properties of lipid membrane (Herold et al., 1987; Veiro et al., 1987; Zeng et al., 1993). Thus, for the purple membrane, alcohol should affect both the structure of the protein and the lipid layer.

In this study, using ethanol to perturb the rigid structure of the purple membrane, the molecular motion of retinal was measured by absorption anisotropy. Fluorescence anisotropy was also employed to examine the effect of ethanol on membrane fluidity. We observed wavelength-dependent absorption anisotropies and an increase in membrane fluidity with the addition of ethanol. Our observations suggest the appearance of a characteristic motion of whole protein within the perturbed purple membrane. We will discuss the molecular motion of bR within the membrane, especially the difference in motion between photointermediates and nonexcited bR.

MATERIALS AND METHODS

Materials

Purple membrane was isolated from *H. salinarium* strain S9 by the standard method (Becher and Cassim, 1975). DPH (1,6-diphenyl-1,3,5-hexatriene) was obtained from Sigma Chemical Co. (St. Louis, MO), and other chemicals were analytical grade. A buffer solution used for all measurements was sodium phosphate, 10 mM, pH 6.9.

Absorption anisotropy measurements

A computer-controlled flash-photolysis apparatus was constructed to obtain absorption anisotropy. The actinic light source (532 nm, 7 ns) was the second harmonic of the fundamental beam of the Q-switched Nd-YAG laser (DCR-2; Quanta-Ray). This actinic laser flash was polarized vertically with a Glan laser polarizer (PLU-10; Optics for Research) placed just in front of the sample cell (10 × 10-mm quartz cuvette), and the repetition rate of the flash was 0.5–0.6 Hz. The absorbance value of the sample was 0.8–0.9 at 570 nm, and the temperature was kept at 20°C. The source of monitoring light was a 120-W halogen lamp, and the beam of monitoring light was perpendicular to that of the actinic flash. The photomultiplier (R2949; Hamamatsu photonics) was used to detect the monitoring light passing through the sample. To select the measuring wavelength and exclude the scattered actinic flash from the sample, two monochromators were placed in the rear of the monitoring light source and in front of the photomultiplier. Sheet polarizers were placed in front of and behind the sample. These polarizers were rotated 90° to change the polarized orientation of the monitoring light.

The output of the photomultiplier was amplified and filtered by a home-built *I-V* converter with an offset voltage (~10-μs response time). The amplified signal was stored in a personal computer equipped with an A/D converter (12-bit resolution, 0.2 ms per point). The offset voltage of the *I-V* converter was adjusted so that its output changed within the input range of the A/D converter (±1 V). In the computer, the stored data were averaged and converted to absorption change. At each measuring wavelength, two components of the absorption changes ($\Delta A^{\parallel}(t, \lambda)$ and $\Delta A^{\perp}(t, \lambda)$) were obtained with the monitoring lights polarized parallel and perpendicular to the polarized orientation of the actinic flash, respectively. The data collection of 100 times was one set of measurements. This set of measurements was performed alternately for two components ($\Delta A^{\parallel}(t, \lambda)$, $\Delta A^{\perp}(t, \lambda)$, $\Delta A^{\parallel}(t, \lambda)$, $\Delta A^{\perp}(t, \lambda)$, etc.). The total repetition time for one component was 200–300. Before each set of measurements, the sample was light-adapted by exposure to continuous yellow light.

Using the measured absorption changes, the absorption anisotropies were calculated as

$$r(t, \lambda) = \frac{\Delta A^{\parallel}(t, \lambda) - \Delta A^{\perp}(t, \lambda)}{\Delta A^{\parallel}(t, \lambda) + 2\Delta A^{\perp}(t, \lambda)} \quad (1)$$

Here the denominator ($\Delta A^{\parallel}(t, \lambda) + 2\Delta A^{\perp}(t, \lambda)$) is independent of the motion of absorption dipoles, and so this value reflects exactly the changes in populations of photointermediates and ground-state bR. The curve of the denominator must be similar to that of the absorption change measured by the monitoring light, which is polarized in the magic angle (54.74°) respect to vertical orientation. However, inadequate setup of optical components lessened the similarity and gave a systematic error in the obtained anisotropy. Thus we took care to correct the polarized orientation of lights and the alignment of optical components. Particular care was taken to arrange all optical components so that the lights passed horizontally and linearly. Then we obtained the fine similarity between the denominator in Eq. 1 and the absorption change measured with the monitoring light polarized in the magic angle.

With increasing intensity of monitoring light, the output of photomultiplier increases, and so it is possible to reduce the voltage applied to the photomultiplier. This reduction of the voltage is very useful for improving the signal-to-noise ratio of the measured absorption change. Thus a lens was placed close to the halogen lamp of the monitoring light source, so that a large amount of light impinged on the monochromator. We confirmed that the measured absorption changes were not distorted with the light intensity used. Reduction of the monitoring light intensity decreased the signal-to-noise ratio but did not modify the measured absorption change. A high intensity of actinic flash also improves the signal-to-noise ratio. However, an increase in flash intensity causes the saturation of excited molecules, and the initial value of anisotropy becomes small. The small initial value of anisotropy results in a small change in the anisotropy. We then adjusted the flash intensity to activate ~6% bR in the sample. Under these conditions, the initial values of obtained anisotropies were ~0.3. Although the reduction of flash intensity increased the initial values of anisotropies, the rates of anisotropy changes with time were independent of the flash intensity.

For the measurement at each concentration of ethanol, the sample was prepared with flesh bR. The bleach of the sample by actinic flash and monitoring light was negligible and did not affect the measured anisotropies. At each concentration of ethanol, the sample was exposed to 1400 flashes for the complete set of measurements of anisotropies. The absorbance value of the sample at 570 nm was not influenced by the set of measurements. Furthermore, the measured anisotropies before and after the complete set of measurements coincided with each other.

Incorporation of DPH into the purple membrane

To examine the fluidity of the purple membrane, we measured the molecular motion of 1,6-diphenyl-1,3,5-hexatriene (DPH) incorporated into the purple membrane. DPH is a rod-shaped fluorophore. When DPH is embedded in the biological or synthetic membranes, it exhibits a wobbling motion that closely reflects the motion of neighboring lipid hydrocarbon chains. The incorporation of DPH into the membrane was performed by adding a few microliters of the DPH concentrated solution in tetrahydrofuran (2 mM) to a few milliliters of the purple membrane suspension. This suspension was incubated for 15 min at 35°C. The final molar ratio of bR to DPH was ~2.8. The concentration of bR in the purple membrane suspension was estimated from a molar extinction coefficient at 568 nm of 63,000.

Fluorescence anisotropy measurements

The picosecond time-resolved fluorescence anisotropy measurements were performed with a time-correlated single photon counting system. The light source for excitation was a cavity dumped dye laser (model 700; Coherent) pumped by synchronized mode-locked Ar ion laser (Innova 100; Coherent). The second harmonic of the fundamental beam of the dye laser was used as the excitation light. The excitation wavelength used was 335 nm (6 ps), and the fluorescence was detected at 430 nm. The details of this apparatus were reported previously (Saito et al., 1991). The temperature was kept at 20°C.

When rod-shaped fluorophores undergo wobbling motion in the lipid bilayer, the fluorescence anisotropy ($r(t)$) is expressed approximately as follows (Kawato et al., 1977):

$$r(t) = (r_0 - r_\infty)\exp(-t/\phi) + r_\infty \quad (2)$$

We determined these parameters (r_0, r_∞, ϕ) by least-squares fits. The wobbling motion of the fluorophores was characterized according to the wobbling-in-cone model, with the cone angle for the wobbling motion, θ_C, and the wobbling diffusion constant, D_W (Kinosita et al., 1977; Lipari and Szabo, 1980). These values were calculated from the following equations:

$$r_\infty/r_0 = [\cos\theta_C(1 + \cos\theta_C)]^2/4 \quad (3)$$

$$\frac{D_W\phi(r_0 - r_\infty)}{r_0} = -\frac{\chi^2(1+\chi)^2\{\ln[(1+\chi)/2] + (1-\chi)/2\}}{2(1-\chi)} + \frac{(1-\chi)(6 + 8\chi - \chi^2 - 12\chi^3 - 7\chi^4)}{24} \quad (4)$$

where $\chi = \cos\theta_C$. Moreover, we calculated the membrane viscosity (η) using the Stokes-Einstein equation:

$$D_W = \frac{kT}{6\eta V_{eff}} \quad (5)$$

where k, T, and V_{eff} denote the Boltzmann constant, absolute temperature, and effective volume of the fluorescent molecule.

RESULTS

Absorption anisotropies in the absence of ethanol

Fig. 1 shows flash-induced absorption anisotropies of the purple membrane aqueous suspension. The selected wavelengths for the measurements of absorption anisotropies were 410, 570, and 680 nm. At these respective wavelengths, the M-intermediate, ground-state bR, and the O-intermediate are mainly monitored. At 680 nm, the summed absorption change ($\Delta A^{\parallel}(t, 680) + 2\Delta A^{\perp}(t, 680)$), the denominator in Eq. 1, increases from an initial negative value due to the contribution of the absorption of ground-state bR (Fig. 1, *inset*). Thus plotting of the anisotropy at 680 nm was started after the absorption change crossed the zero value. As shown in Fig. 1, the time courses of the anisotropy decay at these three wavelengths are almost the same. This slow decay is consistent with those in previous reports (Cherry et al., 1977; Kouyama et al., 1981), in which the changes in absorption anisotropies were interpreted as the rotational motion of the purple membrane itself, not as the motion of retinal within the membrane. The similar decay between observed anisotropies at these three wavelengths suggests that the motion of retinal within the membrane is almost absent in ground-state bR and photointermediates.

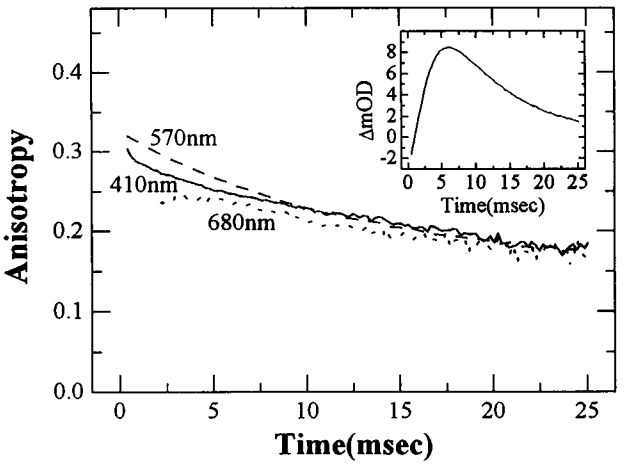

FIGURE 1 Absorption anisotropies of the purple membrane suspension without ethanol. The measured wavelengths are 410, 570, and 680 nm, which are denoted in the figure, and the measurements were performed at 20°C. The anisotropies measured at these three wavelengths have almost the same time dependencies. (*Inset*) The summed absorption change at 680 nm. This value ($\Delta A^{\parallel}(t, 680) + 2\Delta A^{\perp}(t, 680)$) corresponds to the denominator in Eq. 1.

Absorption anisotropies in the presence of ethanol

Fig. 2 shows the anisotropy changes at these selected wavelengths in the presence of various concentrations of ethanol. The absorption spectra of the samples were not affected by the low concentration used in this study (data not shown). Contrary to the results obtained in the absence of ethanol, we observed wavelength- and ethanol concentration-dependent anisotropy changes. At 410 nm (Fig. 2 *A*), the anisotropies do not decay but increase with time. The anisotropy increase is enhanced as the ethanol concentration increases. At 570 nm (Fig. 2 *B*), the decay of the anisotropies becomes rapid with increasing concentration of ethanol, and the anisotropies finally take negative values. At 680 nm (Fig. 2 *C*), the anisotropies show small but distinct changes with the

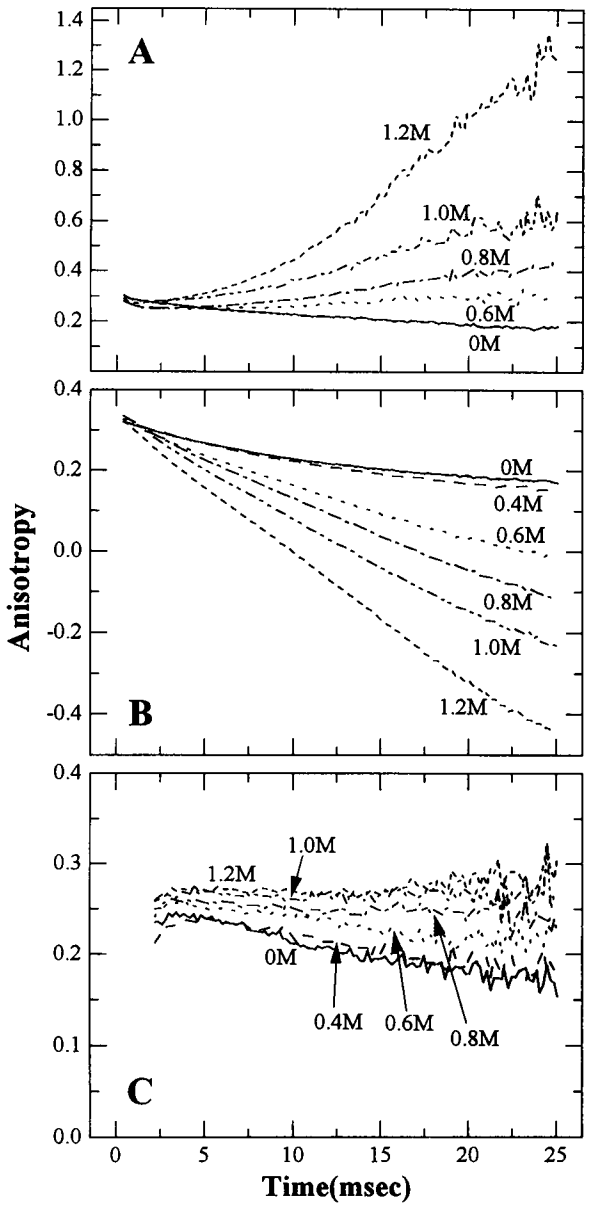

FIGURE 2 Absorption anisotropies of the purple membrane suspension with various concentrations of ethanol. The ethanol concentrations are denoted in the figures. The measurements were performed at 20°C. (*A*) Data obtained at 410 nm. Above 0.8 M ethanol, the anisotropies rise with time and exceed the initial values. (*B*) Data at 570 nm. The decay of the anisotropy becomes rapid with increasing ethanol concentration. (*C*) Data at 680 nm. The anisotropies show small but distinct changes.

addition of ethanol. These characteristic anisotropy changes indicate that the molecular motion of retinal should occur within the membrane, and that the rates of motion are different between ground-state bR and photointermediates.

Fluidity change in the purple membrane by ethanol

The effect of ethanol on membrane fluidity was examined by DPH fluorescence depolarization. As shown in Fig. 3,

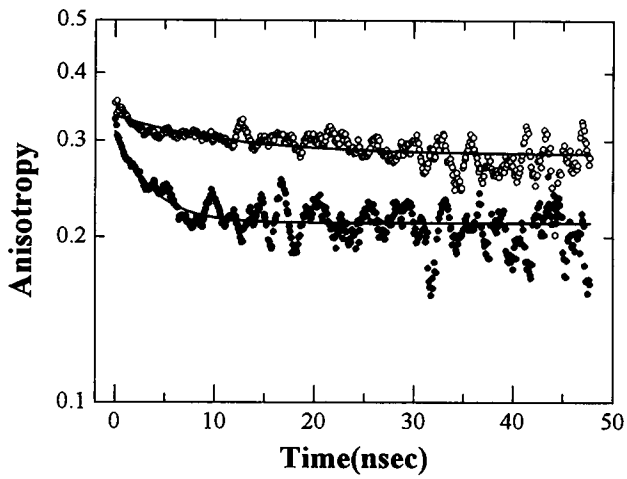

FIGURE 3 Time courses of fluorescence anisotropies of DPH embedded in the purple membrane. ○, Purple membrane suspension without ethanol; ●, with 1.27 M ethanol. The measurements were performed at 20°C. Smooth lines are calculated best-fit curves using Eq. 2. The addition of ethanol induces the rapid decay of the anisotropy.

the decay of the fluorescence anisotropy accelerated with the addition of ethanol. The values of r_0, r_∞, and ϕ in Eq. 2 were obtained by curve fitting analysis with the least-squares method. The cone angle (θ_C), the wobbling diffusion rate (D_W), and the membrane viscosity (η) were calculated using Eqs. 3, 4, and 5; these values are listed in Table 1. The value of effective volume of DPH (V_{eff}) was determined according to the previously reported value (1.5×10^{-22} cm^3) (Kawato et al., 1977). In the absence of ethanol, the wobbling motion of DPH is slow and restricted, as shown in Table 1. The rigid crystalline lattice should hinder the motion of both lipid and bR. However, the mobility of DPH is significantly enhanced by the addition of ethanol. This increased fluidity of the membrane is considered to induce the motion of retinal within the membrane.

DISCUSSION

We observed wavelength-dependent absorption anisotropies in the presence of ethanol. If the orientation of retinal were the same between ground-state bR and photointermediates, the anisotropies should not depend on the measuring wavelength. Thus the motion of retinal must be induced by the addition of ethanol. This retinal motion should change during the photochemical cycle, so that retinal should assume a different orientation between ground-state bR and photoin-

TABLE 1 Fluorescence depolarization parameters of DPH within the purple membranes in the absence or presence of ethanol at 20°C

Ethanol conc. (M)	r_0	r_∞	ϕ (ns)	D_W (10^6 s^{-1})	θ_C (°)	η (poise)
0	0.33	0.28	10.8	2.8	18.8	16.0
1.27	0.31	0.21	3.3	20.0	28.7	2.2

termediates. The rotation of the purple membrane itself does not contribute to the difference in the retinal motion between ground-state bR and photointermediates, and so the motion of retinal occurs within the purple membrane. The retinal motion within the membrane is considered to be the wobbling motion of retinal inside the protein and/or the rotation of the whole protein. The wobbling motion of retinal should be its Brownian motion or the motion that accompanies the wobbling of peptide chains around retinal. The time range of this motion is usually from picoseconds to nanoseconds (Suzuki et al., 1989). The wobbling motion of retinal might be enhanced because the addition of ethanol disrupts the hydrogen bonds between the helix coils. However, our observed anisotropy changes occurred in the millisecond time range. Thus the motion of retinal in the protein is not likely for the origin of the observed anisotropy changes. The rotational motion of the whole protein becomes the most feasible origin of the retinal motion within the purple membrane. As shown in Table 1, the molecular motion of DPH, which was incorporated into the purple membrane, was activated by the addition of ethanol. Like that of DPH, the rotational motion of bR within the purple membrane should be also activated.

The usual extent of the measured anisotropy is $0 \leq r \leq 0.4$. However, our observed anisotropies exceeded this. To understand these characteristic anisotropies, it is essential to obtain individual time courses of the absorption anisotropies for ground-state bR and photointermediates. Three intermediates, M, N, and O, are known to appear sequentially in the millisecond time range. With neutral pH as our measuring condition, the amount of accumulation of N-intermediate is small, and M- and O-intermediates are mainly monitored. In the presence of ethanol, however, Fukuda and Kouyama (1992) reported the accumulation of the N-intermediate. They performed the measurements up to 7 M ethanol. Although their results showed that the alteration of kinetics was exponential with increased concentration of ethanol, at the low concentration of ethanol used in our study, the change was small. We examined the ethanol effect by analyzing the absorption change at 600 nm. This wavelength is the isobestic point between ground-state bR and the O-intermediate (Váró and Lanyi, 1991), and so the photochemical cycle can simply be regarded as bR $\rightarrow$ M $\rightarrow$ N $\rightarrow$ bR at 600 nm. In the absence of ethanol, the measured absorption change was expressed by one exponential curve. If the build-up of the N-intermediate had become significant by the addition of ethanol, two exponential curves would have been needed to fit the measured absorption change. As the concentration of ethanol was increased, the decay of absorption changes accelerated, which corresponded to the increase in the decay rate of the M-intermediate. However, the absorption change at 1.2 M ethanol (the maximum concentration used in the measurement of absorption anisotropies) could be still fitted with one exponential curve. This result showed the accumulation of the N-intermediate to still be negligible at 1.2 M ethanol. Thus we analyzed our data, taking account of three species, ground-state bR, M-, and O-intermediates. Then the summed absorption change at λ nm ($\Delta A(t, \lambda)$), which corresponds to the denominator of Eq. 1, is expressed as follows:

$$\begin{aligned}\Delta A(t, \lambda) &= \Delta A^{\parallel}(t, \lambda) + 2\Delta A^{\perp}(t, \lambda) \\ &= \Delta A_{\mathrm{M}}(t, \lambda) + \Delta A_{\mathrm{bR}}(t, \lambda) + \Delta A_{\mathrm{O}}(t, \lambda) \\ &= \alpha(\lambda)\Delta A_{\mathrm{M}}(t, 410) + \beta(\lambda)\Delta A_{\mathrm{bR}}(t, 570) \\ &\quad + \gamma(\lambda)\Delta A_{\mathrm{O}}(t, 680)\end{aligned} \tag{6}$$

where

$$\alpha(\lambda) = \frac{\epsilon_{\mathrm{M}}(\lambda)}{\epsilon_{\mathrm{M}}(410)}, \quad \beta(\lambda) = \frac{\epsilon_{\mathrm{bR}}(\lambda)}{\epsilon_{\mathrm{bR}}(570)}, \quad \gamma(\lambda) = \frac{\epsilon_{\mathrm{O}}(\lambda)}{\epsilon_{\mathrm{O}}(680)} \tag{7}$$

The terms $\Delta A_{\Omega}(t, \lambda)$ and $\epsilon_{\Omega}(\lambda)$ (Ω = M, bR, O) are the absorption change induced by Ω species and the extinction coefficient of Ω species at λ nm, respectively. The subscript bR denotes ground-state bR. The absorption change of $\Delta A_{\Omega}(t, \lambda)$ is proportional to the change in population of the Ω species. Using the individual anisotropy of Ω species ($r_{\Omega}(t)$), the absorption anisotropy at λ nm ($r(t, \lambda)$) is written as

$$r(t, \lambda) = \frac{\begin{aligned}&\alpha(\lambda)\Delta A_{\mathrm{M}}(t, 410)r_{\mathrm{M}}(t) + \beta(\lambda)\Delta A_{\mathrm{bR}}(t, 570)r_{\mathrm{bR}}(t) \\ &\qquad + \gamma(\lambda)\Delta A_{\mathrm{O}}(t, 680)r_{\mathrm{O}}(t)\end{aligned}}{\Delta A(t, \lambda)} \tag{8}$$

We determined the values of α, β, and γ according to the reported absorption spectra (Cao et al., 1991; Váró and Lanyi, 1991) ($\alpha(570) = 0$, $\alpha(680) = 0$, $\beta(410) = 0.22$, $\beta(680) = 0.03$, $\gamma(410) = 0.25$ and $\gamma(570) = 0.75$) and calculated $r_{\Omega}(t)$ with Eqs. 6 and 8. Calculated anisotropies for M- and O-intermediates are shown in Fig. 4, *A* and *C*, respectively. The time courses of these anisotropies are the same and are superimposable on those obtained without ethanol (Fig. 1). The addition of ethanol increased the membrane fluidity (Table 1), and so the rotational motion of a protein was expected to be facilitated. However, the calculated results show the motion of these two photointermediates to still be restricted, even in the presence of ethanol. On the other hand, the anisotropy of ground-state bR is affected with ethanol, and it takes a negative value above 0.8 M ethanol. The normal rotational motion of a chromophore results in an anisotropy minimum value of zero because the chromophores finally assume a random angular distribution. Thus the negatively deflected change in the anisotropy is due to the remarkable character of ground-state bR.

The absorption change in the photointermediate is positive and proportional to the population of the intermediate, and so its anisotropy expresses the angular distribution of absorption dipoles in the intermediate. The actinic flash is polarized vertically. Thus the initial positive values of anisotropies of photointermediates reflect the vertically polarized angular distribution of their absorption dipoles.

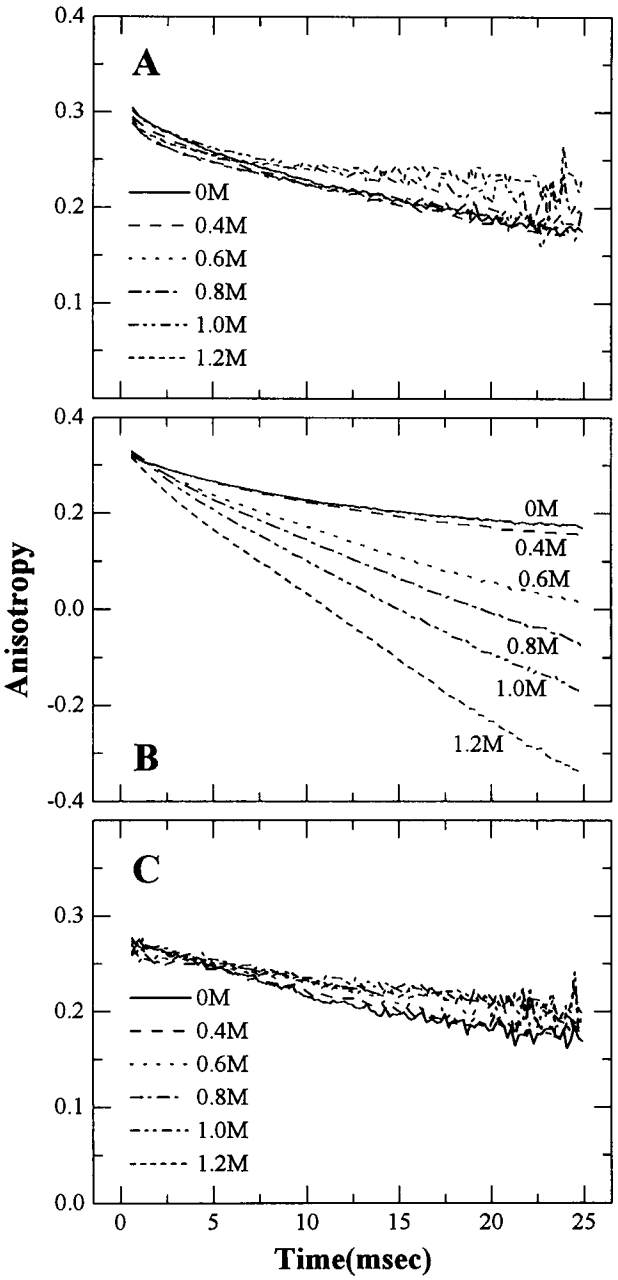

FIGURE 4 Calculated anisotropies attributed only to M-, O-intermediates and ground-state bR with various concentrations of ethanol. The ethanol concentrations are denoted in the figures. The anisotropies of M- (*A*) and O- (*C*) intermediates are independent of the ethanol concentration. With increasing ethanol concentration, only the anisotropy of ground-state bR (*B*) decays rapidly and takes a negative value.

However, the anisotropy of ground-state bR is the exceptional case. The actinic flash causes a depletion of ground-state bR, and so the absorption change of ground-state bR is negative. Thus the anisotropy of ground-state bR expresses that of imaginary "disappeared" molecules. The initial positive value of the anisotropy of ground-state bR corresponds to the horizontally polarized angular distribution of absorption dipoles in ground-state bR. The anisotropy change of ground-state bR, from positive to negative, means that the horizontally polarized distribution shifts to the vertically polarized one through the random one.

To take the analysis further, we should direct our attention to the fact that the absolute absorbance of ground-state bR is contributed by two species of bR, nonexcited bR and "returned" bR. Here "returned" bR is ground-state bR that had been excited by the flash and finished the photochemical cycle. If the mobility of nonexcited bR is different from that of "returned" bR, this difference should affect the anisotropy of ground-state bR. Here we examined the effect of the individual mobilities of these two species on the anisotropy of ground-state bR. As shown in the Appendix, we can express the anisotropy of ground-state bR as follows:

$$r_{bR}(t) = r_{bR}(0) \cdot \frac{r_M(t)}{r_M(0)} \cdot \frac{\Delta A_{bR}(0, 570)\langle P_2(\Delta\theta_{non})\rangle_t + (\Delta A_{bR}(t, 570) - \Delta A_{bR}(0, 570))\langle P_2(\Delta\theta_{re})\rangle_t}{\Delta A_{bR}(t, 570)} \quad (9)$$

where $P_2(\alpha) = (3\cos^2\alpha - 1)/2$ is the second Legendre polynomial and $\langle P_2(\alpha)\rangle_t$ denotes an average of $P_2(\alpha)$ at time t. The terms $\Delta\theta_{non}$ and $\Delta\theta_{re}$ express the displacement of absorption dipoles between times t and zero. $\Delta\theta_{non}$ and $\Delta\theta_{re}$ are angular deviations of the absorption dipoles in nonexcited bR and "returned" bR caused by the rotation of whole protein within the membrane. To examine the effect of these angles on the anisotropy of ground-state bR, we introduce the angle $\Delta\varphi_\Omega$ (Ω = non, re), which is defined in the simple case in which all Ω species rotate through the same angle within the membrane. This term, $\Delta\varphi_\Omega$, is related to $\Delta\theta_\Omega$ by

$$\cos^2(\Delta\varphi_\Omega(t)) = \langle\cos^2(\Delta\theta_\Omega)\rangle_t \qquad \Omega = \text{non, re};\quad 0° \le \Delta\varphi_\Omega, \Delta\theta_\Omega \le 90° \quad (10)$$

Substituting Eq. 10 into Eq. 9, r_{bR} is written as follows:

$$r_{bR}(t) = r_{bR}(0) \cdot \frac{r_M(t)}{r_M(0)} \cdot \frac{\Delta A_{bR}(0, 570)P_2(\Delta\varphi_{non}(t)) + (\Delta A_{bR}(t, 570) - \Delta A_{bR}(0, 570))P_2(\Delta\varphi_{re}(t))}{\Delta A_{bR}(t, 570)} \quad (11)$$

According to Eq. 11, we found the value of r_{bR} at 25 ms in 1.2 M ethanol to change the values of $\Delta\varphi_{non}$ and $\Delta\varphi_{re}$. In this calculation, the constant values of 0.32, 0.79, and 18.8 were used for $r_{bR}(0)$, $r_M(25\text{ ms}/r_M(0)$, and $\Delta A_{bR}(0, 570)/\Delta A_{bR}(25\text{ ms}, 570)$, respectively. These values were determined from the data for 1.2 M ethanol. The calculated values of r_{bR} are summarized in Fig. 5. The usual extent of anisotropy is $0 \le r \le 0.4$. As shown in Fig. 5, however, the calculated anisotropies are distributed over a very wide range. This prolonged extent of the anisotropy originates from the fact that the differences in motion between non-

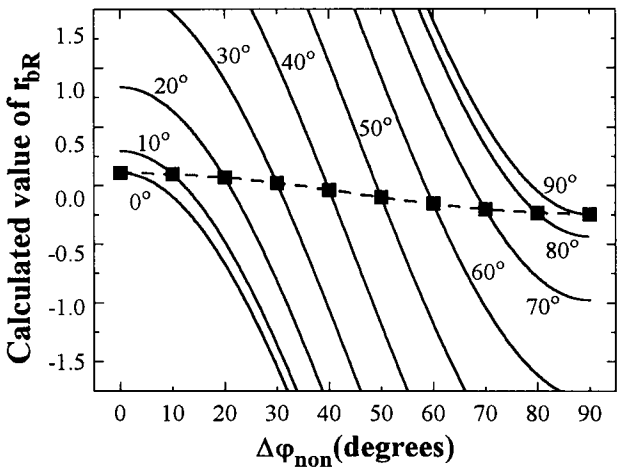

FIGURE 5 Calculated values of the anisotropy of ground-state bR at various rotational angles of nonexcited bR and "returned" bR. These calculations were performed according to Eq. 11. In this calculation, we used the terms of $\Delta\varphi_{non}$ and $\Delta\varphi_{re}$ to express the rotational angles of nonexcited bR and "returned" bR within the membrane, and the values of $\Delta\varphi_{re}$ are denoted in the figure. Other parameters in Eq. 11 were determined from the data at 25 ms in 1.2 M ethanol (see text). The square (■) denotes the case that nonexcited bR and "returned" bR have the same rotational angles ($\Delta\varphi_{non} = \Delta\varphi_{re}$). At each value of $\Delta\varphi_{re}$, the anisotropy of ground-state bR (r_{bR}) becomes small with increasing value of $\Delta\varphi_{non}$. It is noted that the anisotropy value of ground-state bR shown in Fig. 4 *B* (−0.34 at 25 ms in 1.2 M ethanol) is achieved in the case of $\Delta\varphi_{non} > \Delta\varphi_{re}$.

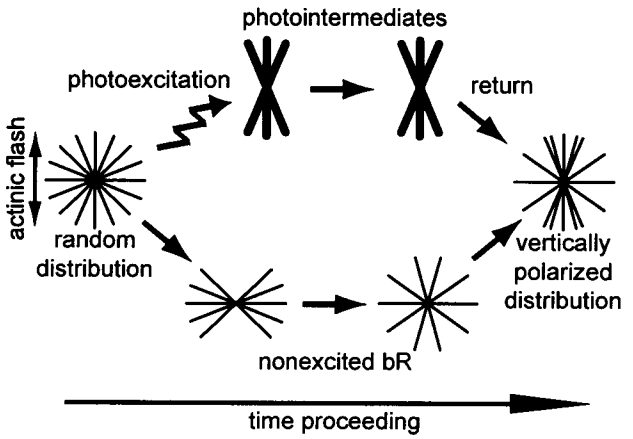

FIGURE 6 The schematic diagram for the motion of absorption dipoles leading the vertically polarized angular distribution of dipoles in all ground-state bR. For ground-state bR, the positive and negative values of the anisotropy correspond to the horizontally and vertically polarized angular distribution of dipoles. The thin and thick lines denote the absorption dipoles of ground-state bR and photointermediates in the sample, respectively. The vertically polarized actinic flash leads the vertically polarized angular distribution of the dipoles in photointermediates, and horizontally polarized distribution in nonexcited bR. When the dipoles of nonexcited bR rotate faster than that of photointermediates, the angular distribution in all ground-state bR polarizes vertically as photointermediates return to ground-state bR.

excited bR and "returned" bR ($\Delta\varphi_{non} \neq \Delta\varphi_{re}$) make it impossible to cancel out the terms of absorption changes in Eq. 11 by division. It is noteworthy that the larger motion of nonexcited bR compared to that of "returned" bR ($\Delta\varphi_{non} > \Delta\varphi_{re}$) induces the negative value of the anisotropy. The same motion of these two species (*squares*) also induces the negative value; however, the minimum value of the anisotropy in this case (−0.13 at $\Delta\varphi_{non} = \Delta\varphi_{re} = 90°$) still does not reach the anisotropy value (−0.34) at 25 ms in 1.2 M ethanol (Fig. 4 *B*). To explain the characteristic anisotropy changes of ground-state bR in Fig. 4 *B*, therefore, the motion of nonexcited bR within the membrane must be larger than that of "returned" bR. The rotation of photointermediates within the membrane is considered to be negligible (Fig. 4, *A* and *C*), and "returned" bR should keep the angular distribution of absorption dipoles in photointermediates. Thus the addition of ethanol must induce the rotation of nonexcited bR within the purple membrane.

Fig. 6 shows a schematic diagram in which the larger rotation of nonexcited bR than that of "returned" bR induces a shift of the horizontally polarized angular distribution of absorption dipoles in all ground-state bR to a vertically polarized one (this shift corresponds to the shift of anisotropy of ground-state bR from positive to negative). Immediately after the excitation with the vertically polarized flash, the angular distributions of absorption dipoles in photointermediates and nonexcited bR are polarized vertically and horizontally, respectively. As shown in Fig. 4, *A* and *C*, the rotation of photointermediates within the membrane is negligibly small. Thus the depolarization of angular distribution in photointermediates is very slow, and the initial vertically polarized distribution is maintained. On the other hand, the rotation of nonexcited bR within the purple membrane makes the absorption dipoles in nonexcited bR assume a more random angular distribution than that in photointermediates. In this situation, the increase in "returned" bR, keeping the vertically polarized distribution in photointermediates, induces the distribution in all ground-state bR to polarize vertically.

To test whether the scheme in Fig. 6 can account for the anisotropy changes of ground-state bR (Fig. 4 *B*), we introduced a simple model for the motion of whole protein within the membrane and performed a fitting analysis. Here we expressed the time dependence of $\langle P_2(\Delta\theta_{non})\rangle_t$ and $\langle P_2(\Delta\theta_{re})\rangle_t$ in Eq. 9. Because the purple membrane is crowded with bR molecules, the proteins should not be able to rotate freely. The rotation of bR molecules is considered to be limited to a certain angle. We expressed $\langle P_2(\Delta\theta_{non})\rangle_t$ as follows:

$$\langle P_2(\Delta\theta_{non})\rangle_t = (1 - A)\exp(-t/\tau) + A \qquad (12)$$

where the constant number A comes from the limitation on the rotation of bR molecules. The extent of value of A must be $0 \leq A \leq 1$. Moreover, we supposed that photointermediates are completely immobilized, and that returned bR begins the identical rotation with nonexcited bR. The absolute value of $\Delta A_{bR}(t, 570)$, which appeared in Eq. 6, is proportional to summed populations of photointermediates at time t. Then $d[\Delta A_{bR}(t, 570)]/dt$ is proportional to the

number of molecules that return to ground-state bR from photointermediates at time t. Thus $\langle P_2(\Delta\theta_{re})\rangle_t$ is expressed as

$$\langle P_2(\Delta\theta_{re})\rangle_t = \frac{d[\Delta A_{bR}(t, 570)]/dt * \langle P_2(\Delta\theta_{non})\rangle_t}{\int_0^t \{d[\Delta A_{bR}(t, 570)]/dt\}} \quad (13)$$

where the numerator is the convolution product. Here we simply expressed $\Delta A_{bR}(t, 570)$ as follows:

$$\Delta A_{bR}(t, 570) = -A_{bR} \exp(-t/\tau_{bR}) \quad (14)$$

Using Eqs. 12 and 14, Eq. 13 can be written as

$$\langle P_2(\Delta\theta_{re})\rangle_t \quad (15)$$

$$= \frac{\int_0^t \frac{A_{bR} \exp(-t'/\tau_{bR})}{\tau_{bR}} \{(1 - A)\exp(-(t - t')/\tau) + A\}\, dt'}{A_{bR}(1 - \exp(-t/\tau_{bR}))}$$

$$= \frac{\{\tau A_{bR}(1 - A)/(\tau_{bR} - \tau)\}\{\exp(-t/\tau_{bR}) - \exp(-t/\tau)\} - A_{bR}A \exp(-t/\tau_{bR}) + A_{bR}A}{A_{bR}(1 - \exp(-t/\tau_{bR}))}$$

Substituting Eqs. 12, 14, and 15 into Eq. 9, we next obtained equation

$$r_{bR}(t) = r_{bR}(0) \cdot \frac{r_M(t)}{r_M(0)} \cdot \left[\frac{1 - A}{\tau_{bR} - \tau}\{\tau_{bR} \exp((1/\tau_{bR} - 1/\tau)t) - \tau\} + A\right] \quad (16)$$

The anisotropy of ground-state bR ($r_{bR}(t)$, Fig. 4 *B*) was fitted to Eq. 16 with the least-squares method, where A and τ were used as fitting parameters. The values used for τ_{bR} were obtained from the fitting of $\Delta A_{bR}(r, 570)$ to Eq. 14, and the values of $r_{bR}(0)$ were constrained to the values determined from Fig. 4 *B*. For $r_M(t)/r_M(0)$, the anisotropy of the M-intermediate at 0 M ethanol (shown in Fig. 4 *A*) was used. The anisotropy change without ethanol was considered to originate from the rotation of the purple membrane itself. Thus, at 0 M ethanol, we supposed both $\langle P_2(\Delta\theta_{non})\rangle_t$ and $\langle P_2(\Delta\theta_{re})\rangle_t$ to be 1. The fitting was performed for the anisotropies of ground-state bR obtained with 0.4–1.2 M ethanol. The fitting results are summarized in Fig. 7 and Table 2. As shown in Table 2, the values of both τ and A decrease continuously with increased ethanol concentration. These results show that the addition of ethanol accelerates the rotation of the bR molecule and loosens the limitation of the rotational angle. Our model is too simple for a precise discussion. Moreover, our model is one of many models that satisfy the scheme in Fig. 6. Therefore, a discussion here about the values of fitting parameters cannot lead to definitive conclusions. However, the parameters took reasonable values and the fitting results simulated well the anisotropies

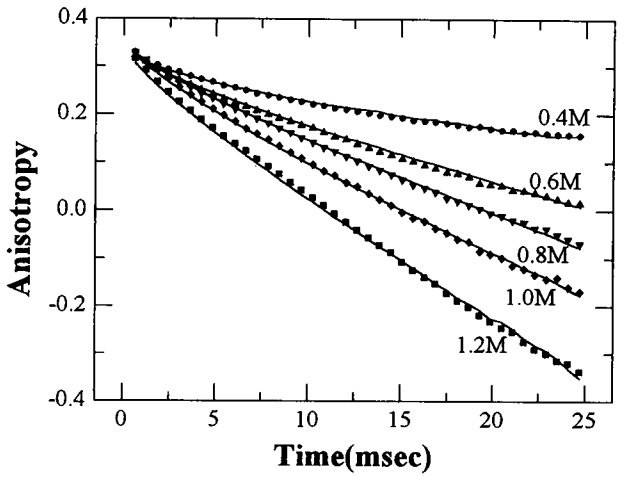

FIGURE 7 The fitting results of anisotropies of ground-state bR with various concentrations of ethanol. The ethanol concentrations are denoted in the figure. The anisotropies of ground-state bR (shown in Fig. 4 *B*) are displayed here with a scatter diagram. These anisotropies were fitted to Eq. 16 with the least-squares method, where A and τ were used as fitting parameters (see text about other parameters in Eq. 16). The determined values of parameters were summarized in Table 2. The solid lines are anisotropies calculated with Eq. 16, using the fitting results.

of ground-state bR. Thus it was confirmed that the scheme in Fig. 6 can account for our measured data.

As shown in Table 1, the addition of ethanol increased the fluidity of the purple membrane. This increase in membrane fluidity is considered to lead to the rotation of nonexcited bR. However, the motion of photointermediates within the membrane is negligible, even in the presence of ethanol. Thus a certain mechanism must restrict the motion of photointermediates. The restricted motion should originate from the conformational change in photointermediates. The conformational change may increase the unit volume for the rotor. Such an increase in the protein volume may become an obstacle to the rotation of the photointermediate among neighboring proteins. The change in the protein volume was reported by Subramaniam et al. (1993). They showed an increase in the protein volume at the M-intermediate. In the kinetics of the photochemical cycle, a cooperative phenomenon was reported. The increase in the flash intensity slowed the decay rate of the absorption change of the M-intermediate. Thus the conformation change in excited bR was considered to affect the photochemical cycle of neighboring protein (Dancsházy and Tokaji, 1993; Tokaji,

TABLE 2 Fitting parameters for the anisotropies of ground-state bR with various concentrations of ethanol

Ethanol conc. (M)	r_{bR} (0)	τ_{bR} (ms)	τ (ms)	A
0.4	0.32	9.9	12.4	0.93
0.6	0.33	8.2	11.5	0.72
0.8	0.34	8.1	11.2	0.60
1.0	0.33	8.3	10.7	0.43
1.2	0.32	8.1	10.7	0.17

1993, 1995; Hendler et al., 1994; Mukhopadhyay et al., 1994). Váró et al. (1996) suggested that the expansion of protein volume in excited bR increases the lateral pressure within the purple membrane, and the pressure influences the kinetics of the photochemical cycle of neighboring protein. Our observed restriction of the rotation of photointermediates may be a dynamic property relating to this cooperative phenomenon.

The changed conformation in the outer part of the photointermediate may also lead to binding interaction with neighboring proteins. The binding interaction increases the unit volume for the rotor. Other proteins around the interacting proteins should become obstacles to the rotation of such a large unit. In animals, the retinylidene proteins commonly function as the visual pigment. The phototaxis receptors in *H. salinarium* are the retinylidene proteins sensoryrhodopsin and phoborhodopsin. The conformational changes in the outer parts of these proteins are essential for activating signal-transducing proteins. The conformational change of bR may also induce interaction with neighboring proteins, and this protein-protein interaction may restrict the motion of photointermediates.

For D96N bR, we observed a slower rotational motion for the M-intermediate than for nonexcited bR (Kikukawa et al., 1995). The site-specific mutation should affect the protein conformation, and the changed conformation may perturb the purple membrane. Thus the difference in motion between nonexcited bR and M-intermediate should be measurable. Perturbation of the purple membrane of wild-type bR by the addition of ethanol is considered to be similar to that caused by the site-specific mutation. Within the purple membrane of wild-type bR, the packing of proteins may be so tight that protein motion is severely restricted. This tight packing was loosened by the addition of ethanol, which was confirmed by the increase in membrane fluidity. The perturbation of the purple membrane should enable nonexcited bR to rotate. Then the restriction of motion of photointermediates originating from their conformational changes should become measurable.

APPENDIX

Separating the contributions of nonexcited bR and "returned" bR, we will formulate the absorption anisotropy of ground-state bR (r_{bR}). Because the absorption change induced by ground-state bR ($\Delta A_{bR}(t, \lambda)$) is negative, r_{bR} shows the anisotropy of imaginary "disappeared" molecules. The anisotropy of "existing" ground-state bR, r^R_{bR}, is written as

$$r^R_{bR}(t) = \frac{(A_{570} + \Delta A^{\parallel}_{bR}(t, 570)) - (A_{570} + \Delta A^{\perp}_{bR}(t, 570))}{(A_{570} + \Delta A^{\parallel}_{bR}(t, 570)) + 2(A_{570} + \Delta A^{\perp}_{bR}(t, 570))} \tag{17}$$

where A_{570} is the absorbance value of the sample at 570 nm, and $\Delta A^{\parallel}_{bR}(t, 570)$ and $\Delta A^{\perp}_{bR}(t, 570)$ are absorption changes induced by ground-state bR at 570 nm with the monitoring lights polarized in parallel and perpendicular to the polarized orientation of the actinic flash. Then r_{bR} is related to r^R_{bR} by

$$r_{bR}(t) = r^R_{bR}(t) \cdot \frac{3A_{570} + \Delta A_{bR}(t, 570)}{\Delta A_{bR}(t, 570)} \tag{18}$$

where $\Delta A_{bR}(t, 570)$ is $\Delta A_{bR}(t, 570) = \Delta A^{\parallel}_{bR}(t, 570) + 2\Delta A^{\perp}_{bR}(t, 570)$ and is independent of the angular distribution of absorption dipoles. Using the anisotropies of nonexcited bR (r_{non}) and "returned" bR (r_{re}), r^R_{bR} can be written as follows:

$$r^R_{bR}(t) = \frac{(3A_{570} + \Delta A_{bR}(0, 570))r_{non}(t) + (\Delta A_{bR}(t, 570) - \Delta A_{bR}(0, 570))r_{re}(t)}{3A_{570} + \Delta A_{bR}(t, 570)} \tag{19}$$

where $(3A_{570} + \Delta A_{bR}(0, 570))$ and $(\Delta A_{bR}(t, 570) - \Delta A_{bR}(0, 570))$ correspond to the populations of nonexcited bR and "returned" bR, respectively.

We introduce the terms $\Delta\theta_{non}$, $\Delta\theta_{re}$, and $\Delta\theta_m$ to express the angular deviations of absorption dipoles at times t and zero. The angles $\Delta\theta_{non}$ and $\Delta\theta_{re}$ indicate, respectively, the angular deviations of nonexcited bR and "returned" bR caused by the rotation of protein within the membrane, and $\Delta\theta_m$ indicates the angular deviation of both species caused by the rotation of the membrane itself. We next obtain the equation

$$r_\Omega(t) = r_\Omega(0) \cdot \langle P_2(\Delta\theta_\Omega)\rangle_t \cdot \langle P_2(\Delta\theta_m)\rangle_t$$
$$\Omega = \text{non, re;} \quad 0° \le \Delta\theta_\Omega, \Delta\theta_m \le 90° \tag{20}$$

where $P_2(\alpha) = (3\cos^2\alpha - 1)/2$ is the second Legendre polynomial, and $\langle\ \rangle_t$ is the average of $P_2(\Delta\theta_\Phi)$ (Φ = non, re, m) for all nonexcited bR or all "returned" bR or both species at time t.

At time 0, $\Delta\theta_{non}$, $\Delta\theta_{re}$, and $\Delta\theta_m$ are 0°, and $r_{re}(0)$ expresses the angular distribution of absorption dipoles in the excited bR immediately after the flash excitation. Because the angular distribution for all molecules (including nonexcited bR and excited bR) at time 0 is random, the anisotropy of all molecules is zero. Using $r_{non}(0)$ and $r_{re}(0)$, the anisotropy of all molecules is expressed as follows:

$$\frac{(3A_{570} + \Delta A_{bR}(0, 570))r_{non}(0) - \Delta A_{bR}(0, 570)r_{re}(0)}{(3A_{570} + \Delta A_{bR}(0, 570)) - \Delta A_{bR}(0, 570)} = 0 \tag{21}$$

where $(3A_{570} + \Delta A_{bR}(0, 570))$ and $-\Delta A_{bR}(0, 570)$ correspond, respectively, to the populations of nonexcited bR and excited bR at time 0. Furthermore, at time 0, the anisotropy of "existing" ground-state bR ($r^R_{bR}(0)$) coincides with that of nonexcited bR ($r_{non}(0)$). On the other hand, the anisotropy of the imaginary "disappeared" molecules ($r_{bR}(0)$) coincides with that of excited bR, thus,

$$r_{bR}(0) = r_{re}(0) \tag{22}$$

As shown in Fig. 4, *A* and *C*, the decay of anisotropies of photointermediates should originate from the rotation of the membrane itself. Thus we used r_M (anisotropy of the M-intermediate) as the anisotropy change induced exactly by the rotation of membrane itself. Using r_M, $\langle P_2(\Delta\theta_m)\rangle_t$ can be written as

$$\langle P_2(\Delta\theta_m)\rangle_t = r_M(t)/r_M(0) \tag{23}$$

Substituting Eqs. 19–23 into Eq. 18, we obtain r_{bR} as follows:

$$r_{bR}(t) = r_{bR}(0) \cdot \frac{r_M(t)}{r_M(0)} \cdot \frac{\Delta A_{bR}(0, 570)\langle P_2(\Delta\theta_{non})\rangle_t + (\Delta A_{bR}(t, 570) - \Delta A_{bR}(0, 570))\langle P_2(\Delta\theta_{re})\rangle_t}{\Delta A_{bR}(t, 570)} \tag{24}$$

We thank Prof. K. Inoue and Dr. A. Yamanaka for allowing us to use their Q-switched Nd-YAG laser and for helpful discussions.

REFERENCES

Ahl, P. L., and R. A. Cone. 1984. Light activates rotations of bacteriorhodopsin in the purple membrane. *Biophys. J.* 45:1039–1049.

Becher, B., and J. Y. Cassim. 1975. Improved isolation procedures for the purple membrane of *Halobacterium halobium*. *Prep. Biochem.* 5:161–178.

Cao, Y., G. Váró, M. Chang, B. Ni, R. Needleman, and J. K. Lanyi. 1991. Water is required for proton transfer from aspartate-96 to the bacteriorhodopsin Schiff base. *Biochemistry.* 30:10972–10979.

Cherry, R. J., M. P. Heyn, and D. Oesterhelt. 1977. Rotational diffusion and exciton coupling of bacteriorhodopsin in the cell membrane of *Halobacterium halobium*. *FEBS Lett.* 78:25–30.

Dancsházy, Z., and Z. Tokaji. 1993. Actinic light density dependence of the bacteriorhodopsin photocycle. *Biophys. J.* 65:823–831.

El-Sayed, M. A. 1992. On the molecular mechanisms of the solar to electric energy conversion by the other photosynthetic system in nature, bacteriorhodopsin. *Acc. Chem. Res.* 25:279–286.

Fukuda, K., and T. Kouyama. 1992. Formation and decay kinetics of bacteriorhodopsin's N intermediate: softening the protein conformation with alcohols affects intra-protein proton transfer and retinal isomerization. *Photochem. Photobiol.* 56:1057–1062.

Henderson, R., J. M. Baldwin, T. A. Ceska, F. Zemlin, E. Beckmann, and K. H. Downing. 1990. Model for the structure of bacteriorhodopsin based on high-resolution electron cryo-microscopy. *J. Mol. Biol.* 213: 899–929.

Henderson, R., and P. N. T. Unwin. 1975. Three-dimensional model of purple membrane obtained by electron microscopy. *Nature.* 257:28–32.

Hendler, R. W., Z. Dancsházy, S. Bose, R. I. Shrager, and Z. Tokaji. 1994. Influence of excitation energy on the bacteriorhodopsin photocycle. *Biochemistry.* 33:4604–4610.

Herold, L. L., E. S. Rowe, and R. G. Khalifah. 1987. ^{13}C-NMR and spectrophotometric studies of alcohol-lipid interactions. *Chem. Phys. Lipids.* 43:215–225.

Kawato, S., K. J. Kinosita, and A. Ikegami. 1977. Dynamic structure of lipid bilayers studied by nanosecond fluorescence techniques. *Biochemistry.* 16:2319–2324.

Kikukawa, T., T. Araiso, K. Mukasa, T. Shimozawa, and N. Kamo. 1995. The molecular motion of bacteriorhodopsin mutant D96N in the purple membrane. *FEBS Lett.* 377:502–504.

Kinosita, K. J., R. Kataoka, Y. Kimura, O. Gotoh, and A. Ikegami. 1981. Dynamic structure of biological membranes as probed by 1,6-diphenyl-1,3,5-hexatriene: a nanosecond fluorescence depolarization study. *Biochemistry.* 20:4270–4277.

Kinosita, K. J., S. Kawato, and A. Ikegami. 1977. A theory of fluorescence polarization decay in membranes. *Biophys. J.* 20:289–305.

Korenstein, R., and B. Hess. 1978. Immobilization of bacteriorhodopsin and orientation of its transition moment in purple membrane. *FEBS Lett.* 89:15–20.

Kouyama, T., Y. Kimura, K. J. Kinosita, and A. Ikegami. 1981. Immobility of the chromophore in bacteriorhodopsin. *FEBS Lett.* 124:100–104.

Lanyi, J. K. 1993. Proton translocation mechanism and energetics in the light-driven pump bacteriorhodopsin. *Biochim. Biophys. Acta.* 1183: 241–261.

Lipari, G., and A. Szabo. 1980. Effect of librational motion on fluorescence depolarization and nuclear magnetic resonance relaxation in macromolecules and membranes. *Biophys. J.* 30:489–506.

Mitaku, S., K. Ikuta, H. Itoh, R. Kataoka, M. Naka, M. Yamada, and M. Suwa. 1988. Denaturation of bacteriorhodopsin by organic solvents. *Biophys. Chem.* 30:69–79.

Mukhopadhyay, A. K., S. Bose, and R. W. Hendler. 1994. Membrane-mediated control of the bacteriorhodopsin photocycle. *Biochemistry.* 33:10889–10895.

Oesterhelt, D., J. Tittor, and E. Bamberg. 1992. A unifying concept for ion translocation by retinal proteins. *J. Bioenerg. Biomembr.* 24:181–191.

Otto, H. and M. P. Heyn. 1991. Between the ground- and M-state of bacteriorhodopsin the retinal transition dipole moment tilts out of the plane of the membrane by only 3°. *FEBS Lett.* 293:111–114.

Otto, H., C. Zscherp, B. Borucki, and M. P. Heyn. 1995. Time-resolved polarized absorption spectroscopy with isotropically excited oriented purple membranes: the orientation of the electronic transition dipole moment of the chromophore in the O-intermediate of bacteriorhodopsin. *J. Phys. Chem.* 99:3847–3853.

Rothschild, K. J. 1992. FTIR difference spectroscopy of bacteriorhodopsin: toward a molecular model. *J. Bioenerg. Biomembr.* 24:147–167.

Saito, H., T. Araiso, H. Shirahama, and T. Koyama. 1991. Dynamics of the bilayer-water interface of phospholipid vesicles and the effect of cholesterol: a picosecond fluorescence anisotropy study. *J. Biochem.* 109:559–565.

Sherman, W. V., and S. R. Caplan. 1977. Chromophore mobility in bacteriorhodopsin. *Nature.* 265:273–274.

Sherman, W. V., M. A. Slifkin, and S. R. Caplan. 1976. Kinetic studies of phototransients in bacteriorhodopsin. *Biochim. Biophys. Acta.* 423: 238–248.

Song, Q., G. S. Harms, C. Wan, and C. K. Johnson. 1994. Reorientations in the bacteriorhodopsin photocycle. *Biochemistry.* 33:14026–14033.

Stoeckenius, W., R. H. Lozier, and R. A. Bogomolni. 1979. Bacteriorhodopsin and the purple membrane of halobacteria. *Biochim. Biophys. Acta.* 505:215–278.

Subramaniam, S., M. Gerstein, D. Oesterhelt, and R. Henderson. 1993. Electron diffraction analysis of structural changes in the photocycle of bacteriorhodopsin. *EMBO J.* 12:1–8.

Suzuki, S., S. Kawato, T. Kouyama, K. J. Kinosita, A. Ikegami, and M. Kawakita. 1989. Independent flexible motion of submolecular domains of the Ca^{2+},Mg^{2+}-ATPase of sarcoplasmic reticulum measured by time-resolved fluorescence depolarization of site-specifically attached probes. *Biochemistry.* 28:7734–7740.

Tokaji, Z. 1993. Dimeric-like kinetic cooperativity of the bacteriorhodopsin molecules in purple membranes. *Biophys. J.* 65:1130–1134.

Tokaji, Z. 1995. Cooperativity-regulated parallel pathways of the bacteriorhodopsin photocycle. *FEBS Lett.* 357:156–160.

Váró, G., and J. K. Lanyi. 1991. Kinetic and spectroscopic evidence for an irreversible step between deprotonation and reprotonation of the Schiff base in the bacteriorhodopsin photocycle. *Biochemistry.* 30:5008–5015.

Váró, G., R. Needleman, and J. K. Lanyi. 1996. Protein structural change at the cytoplasmic surface as the cause of cooperativity in the bacteriorhodopsin photocycle. *Biophys. J.* 70:461–467.

Veiro, J. A., P. Nambi, L. L. Herold, and E. S. Rowe. 1987. Effect of *n*-alcohols and glycerol on the pretransition of dipalmitoylphosphatidylcholine. *Biochim. Biophys. Acta.* 900:230–238.

Wan, C., J. Qian, and C. K. Johnson. 1993. Light-induced reorientation in the purple membrane. *Biophys. J.* 65:927–938.

Zeng, J., K. E. Smith, and P. L.-G. Chong. 1993. Effects of alcohol-induced lipid interdigitation on proton permeability in L-α-dipalmitoylphosphatidylcholine vesicles. *Biophys. J.* 65:1404–1414.